Title	Crystallization behavior of electron-beam-evaporated amorphous silicon films on textured glass substrates by flash lamp annealing
Author(s)	Yago, Aimi; Ohdaira, Keisuke
Citation	Thin Solid Films: 138681
Issue Date	2021-04-15
Type	Journal Article
Text version	author
URL	http://hdl.handle.net/10119/18227
Rights	Copyright (C)2021, Elsevier. Licensed under the Creative Commons Attribution-NonCommercial-NoDerivatives 4.0 International license (CC BY-NC-ND 4.0). [http://creativecommons.org/licenses/by-nc-nd/4.0/] NOTICE: This is the author's version of a work accepted for publication by Elsevier. Aimi Yago, Keisuke Ohdaira, Thin Solid Films, 2021, 138681,DOI:10.1016/j.tsf.2021.138681. https://doi.org/10.1016/j.tsf.2021.138681
Description	

Crystallization behavior of electron-beam-evaporated amorphous silicon films on textured glass substrates by flash lamp annealing

Aimi Yago and Keisuke Ohdaira

Japan Advanced Institute of Science and Technology, Nomi, Ishikawa 923-1292, Japan

*E-mail: ohdaira@jaist.ac.jp

Flash lamp annealing (FLA) is one of the short-duration annealing methods suitable for the crystallization of micrometer-order-thick amorphous silicon (a-Si) films for thin-film polycrystalline silicon (poly-Si) solar cells. The crystallization of electron-beam-(EB-) evaporated a-Si films formed on flat glass substrates by FLA is known to take place through explosive crystallization (EC), by which laterally stretched large crystal grains are formed. In this study, we experimentally investigate the behavior of the FLA-induced crystallization of EB-evaporated a-Si films on glass substrates with intentionally roughed surfaces. When a-Si films on the textured glass substrates receive a FL pulse light consisting of sub-pulses with variable emission frequency, macroscopic stripe patterns with a constant width are observed on the poly-Si surface. This indicates the emergence of EC in EB-evaporated a-Si films also on textured glass substrates, similar to the case of a-Si films on flat substrates. Poly-Si films formed on textured glass substrates have smaller Si crystal grains in the vicinity of the Si/glass interface than the grains near the surface. Moreover, the lateral crystallization velocity of a-Si films on texture glass substrates is smaller compared to that on flat glass substrates. These indicate that the behavior of the EC of EB-evaporated a-Si films is affected by the surface morphology of glass substrates.

1. Introduction

Thin-film polycrystalline silicon (poly-Si) solar cells have attracted attention as next-generation solar cells due to their small amount of material usage and resulting potential for lower fabrication cost [1–10]. At present, the record efficiency of thin-film poly-Si solar cell on glass substrates is up to >15% [10]. The formation of thin-film poly-Si films by the crystallization of amorphous Si (a-Si) films using short-duration heat treatment is expected for high productivity. Excimer laser annealing (ELA) has been widely used for the formation of thin poly-Si films particularly for thin-film transistors [11–15]. ELA typically has a pulse duration on the order of 10 ns, corresponding to a thermal diffusion length in a-Si of ~0.1 μm, which is insufficient for the crystallization of micrometer-order-thick a-Si films for solar cell application. Rapid thermal annealing (RTA) has much longer heating duration of several seconds [16–20], by which a thermal diffusion length in a-Si and glass exceeds the thickness of glass substrates (~1 mm). This leads to thermal damage to whole glass substrates. They are thus not suitable for the mass production of thin-film poly-Si on glass substrates. Flash lamp annealing (FLA) is an annealing method using millisecond-order pulse light emitted from a xenon lamp [21–25]. The thermal diffusion lengths in a-Si and glass in millisecond-order annealing are several tens of μm, which is suitable for the formation of thin-film poly-Si while suppressing thermal damage to glass [25]. Besides, large-area a-Si can be crystallized with one flash light just by expanding the irradiation area.

We have thus far reported the crystallization of a-Si films, prepared by catalytic chemical vapor deposition (Cat-CVD), sputtering, and electron-beam (EB) evaporation, by FLA [24–30]. The crystallization of EB-evaporated a-Si films prepared on flat glass substrates progresses through explosive crystallization (EC) governed by liquid-phase epitaxy (LPE), by which crystal grains stretched in several tens of μm in a lateral direction are formed [26]. The emergence of EC has been experimentally confirmed by the formation of macroscopic stripe patterns on the poly-Si films, originating from periodic temperature modulation during FLA [27, 28]. We have also performed the FLA of EB-evaporated a-Si films on textured glass substrates, aiming at the suppression of film cracking and enhancement of light trapping for the application of the poly-Si films to solar cells [30]. Raman spectroscopy revealed that poly-Si films formed from EB-evaporated a-Si films on moderately textured glass substrates have the full width at half maximum (FWHM) of a c-Si peak similar to that of poly-Si on flat glass

substrates, indicating equivalent grain size. The effect of the morphology of glass surface on the behavior of the crystallization of EB-evaporated a-Si films, however, has not been fully clarified yet. EC is governed by heat release due to enthalpy difference between a-Si and c-Si phases and its lateral diffusion. Thus, the roughness of glass substrates might affect the emergence and/or the mode of EC, LPE-based one or solid-phase-based one. In this study, we experimentally investigated the crystallization behavior of EB-evaporated a-Si films on textured glass substrates by FLA.

2. Experimental procedures

We ultrasonically cleaned 19.8×19.8×0.7 mm^3 glass (Corning Eagle XG) substrates using Semico clean 56 (including tetramethylammonium hydroxide), ethanol, and deionized water for 10 minutes, respectively. Textured surfaces on the glass substrates were formed by reactive ion etching (RIE) for 1 h using CF_4 at a flow rate of 30 sccm, a pressure of 2.6 Pa, and an RF power of 200 W. a-Si films with a thickness of ~3 μm were deposited on flat and textured glass substrates by EB evaporation at a substrate temperature of 300 °C.

FLA was performed only once for each EB-evaporated a-Si film at a fluence of 20 J/cm^2, a pulse duration of 7 ms, and a preheating temperature of 500 °C in Ar atmosphere. The millisecond-order flash lamp pulse consisted of many square-wave sub-pulses with an almost constant intensity and an on:off ratio of 4:1. The irradiation of the sub-pulses on Si films resulted in the cyclic modulation of the temperature of the Si films during FLA, by which macroscopic stripe patterns are left behind if lateral EC occurs [27, 28]. Since the width of the macroscopic stripes corresponds to the length of lateral crystallization during one sub-pulse irradiation, we can easily estimate an EC velocity (v_{EC}) from the relationship between the width and the sub-pulse emission frequency. Note that EC continues during the sub-pulse emission is off because the Si film can keep a sufficiently high temperature for the EC [28]. In this study, we modulated the sub-pulse emission frequency in a range of 1–10 kHz.

The surface roughness of the glass substrates was measured on an atomic force microscope (AFM) (Digital Instruments, Nanoscope IIIa) under the tapping mode. The optical reflectance spectra of the Si films before and after FLA was measured by ultraviolet and visible spectrophotometer (Shimadzu, UV-3150) equipped with an integrating sphere. The presence or absence of the crystallization of Si films and their crystallinity before and after

FLA were evaluated by Raman spectroscopy (Renishaw, Ramascope) using the 632.8 nm line of a He-Ne laser. The Raman spectra were obtained at three points for each sample to confirm the uniformity of the crystallization. The microstructures of poly-Si formed by FLA on textured glass substrates were observed in a cross-sectional transmission electron microscope (TEM) (Hitachi, H-9500) at an acceleration voltage of 200 kV. The TEM image for the poly-Si films on flat glass substrates can be seen elsewhere [26].

3. Results

Fig. 1 shows the AFM image of a glass surface after RIE for 1 h. A similar rough surface morphology as our previous work was obtained [30]. Before RIE, the root-mean-square (RMS) roughness of a glass substrate was less than 1 nm, while the RMS roughness increased to 20–40 nm by performing RIE. Fig. 2 shows the optical reflectance spectra of Si films before and after FLA measured from the Si side. The interference shown in the long-wavelength region of the spectra for flat samples disappears in the spectra for the textured samples. This is due to light scattering on the surface of textured glass and is a clear indication of the formation of glass roughness. The reflectance of Si films on the textured glass substrate is 10% lower than that of the Si film on the flat glass substrate. This can contribute to a reduction in a fluence required for the crystallization of EB-evaporated a-Si films [29]. Note that the optical reflectance of the poly-Si film formed on textured glass substrates is also lower than that formed on flat glass substrates. This will lead to anti-reflection and light trapping of incident sunlight if the poly-Si films are applied to solar cells.

Fig. 3 shows the Raman spectra of Si films after FLA, in which the crystallization of all the samples were performed under the same FLA condition with a fluence of ~20 J/cm^2 and a sub-pulse emission frequency of 1 kHz. The peaks originating from crystalline Si (c-Si) phase are clearly seen at ~520 cm^{-1} on the whole area of all the Si films, indicating that the samples are crystallized. Note that the c-Si peaks of the poly-Si films on textured glass substrates are slightly shifted to a high wavenumber than those on flat glass substrates. This may indicate the relaxation of tensile stress by using glass substrates with textured morphology [31]. The FWHM values of the c-Si Raman peaks of all the samples are obtained to be 4–5 cm^{-1}, independent of the presence or absence of textures on glass substrates. These results suggest that the crystallization under the similar behavior takes place both on the flat

and textured glass substrates and these poly-Si films contain crystal grains with similar sizes. We have also confirmed that these features of the Raman spectra of Si films are independent of sub-pulse emission frequency.

Fig. 4 shows the surface images of poly-Si films on flat and textured glass substrates after FLA with sub-pulse emission frequencies of 2, 5, and 10 kHz. The stripe patterns of poly-Si films on textured glass substrates were not clearly seen when the photographs of the poly-Si surfaces were captured in a normal way because of light scattering. We thus photographed the surfaces of poly-Si films on texture glass substrates with white light illumination from the back side of the samples. All the samples shows macroscopic stripe patterns, and the stripe width is decreased with increase in the sub-pulse emission frequency. This clearly demonstrates the emergence of EC also on textured glass substrates [27, 28]. As mentioned above, we can easily estimate the v_{EC} from the relationship between the width of macroscopic stripe patterns and the sub-pulse emission frequency. Fig. 5 shows the width of the macroscopic stripe patterns as a function of the reciprocal of the sub-pulse emission frequency, i.e. duration for one sub-pulse. The slopes of the plots in Fig. 5 thus correspond to v_{EC} [27, 28]. The v_{EC} of Si films on flat and textured glass substrates obtained from the slopes are also indicated in Fig. 5. The EB-evaporated a-Si films on flat glass substrates shows a v_{EC} of ~14 m/s, which is equivalent to the LPE velocity of molten Si near the melting point of a-Si [23] and reproduces our previous results [27, 28]. On the contrary, the estimated v_{EC} on textured glass substrates is smaller than ~14 m/s. This indicates that the behavior of the EC is affected by the presence of textured morphology of glass surfaces.

Fig. 6 shows the cross-sectional TEM images of the poly-Si formed on the textured glass substrate. The cross-section was formed along the EC direction. One can clearly see laterally stretched crystal grains particularly near the poly-Si surface. This indicates the emergence of LPE-based EC. On the contrary, there are smaller grains in the vicinity of the textured glass surface, and the angle of the stretching direction of large grains is different from that near the poly-Si surface. We have also confirmed the difference of grain features in electron diffraction (ED) patterns taking near the poly-Si surface and near the Si/glass interface (not shown here). This seemingly conflicts with the result of Raman spectra, shown in Fig. 3, in which the FWHMs of c-Si peaks similar to that of poly-Si on flat glass substrates are confirmed. This can be explained by the surface-sensitive nature of Raman spectroscopy. Even using a He-Ne

laser with a wavelength of 632.8 nm, corresponding to a penetration depth in c-Si of ~3 μm, the Raman spectra contain smaller contribution from the bottom side, and no significant difference is seen between the spectra of poly-Si on flat and textured glass substrates.

4. Discussion

As mentioned in the previous chapter, the crystallization of EB-evaporated a-Si films by FLA on textured glass substrates is based on EC, successive crystallization driven by the release of heat due to the enthalpy difference between a-Si and c-Si phases and thermal diffusion towards surrounding a-Si [32]. The formation of macroscopic stripe patterns by the irradiation of flash lamp pulse consisting of sub-pulses is the clear experimental evidence for the emergence of EC [27, 28]. The EC of a-Si films induced by FLA can be basically divided into two behaviors. One is LPE-based EC, in which molten Si always exist during the EC and crystallization occurs only through liquid-phase epitaxy [26]. The other is an EC partly involving solid-phase crystallization. In this particular EC, an LPC region and a solid-phase-nucleation region appear alternatively with a microscopic period of ~1 μm [25]. We have clarified, in our previous work using flat glass substrates, that the usage of CVD or sputtered a-Si films as precursors leads to the emergence of the latter EC, while the former LPC-based EC occurs in EB-evaporated a-Si precursors. The v_{EC}'s of these two ECs have been estimated to be ~14 m/s for the former LPC-based EC and ~4 m/s for the latter SPC-involved EC, based on the relationship between the macroscopic stripe patterns formed by the irradiation of sub-pulses and the emission frequency of the sub-pulses [27, 28].

As clarified in Fig. 5, the v_{EC} of EB-evaporated a-Si films on textured glass substrates is close to but slightly smaller than the v_{EC} of EB-evaporated a-Si films on flat glass substrates. This indicates that the behavior of EC is slightly affected by the existence of glass roughness. The effect of textures on the EC behavior can also be confirmed in the TEM images shown in Fig. 6. Relatively small crystal grains can be seen close to the glass surface. This can be explained as follows. As mentioned above, EC progresses laterally by heat release originating from the enthalpy difference between c-Si and a-Si and its lateral thermal diffusion. Under the existence of glass textures, part of generated heat diffuses not into a-Si but into the protrusion of glass, at which heat generation by crystallization does not occur. Molten Si existing between c-Si and a-Si during LPC-based EC may disappear there and solid-phase

crystallization becomes dominant, leading to the formation of smaller crystal grains. The disappearance of molten Si also explains the decrease in v_{EC} in EB-evaporated a-Si on textured glass.

Based on the experimental results and discussion above, we concluded that the EC of EB-evaporated a-Si films takes place on textured glass substrates, but is not completely the same as that on flat glass substrates.

5. Conclusion

We investigated the behavior of the EC, induced by FLA, of EB-evaporated a-Si films on textured glass substrates. We experimentally confirmed the emergence of the EC of EB-evaporated a-Si films on textured glass substrates, by observing the macroscopic stripe patterns formed by the irradiation of the millisecond pulse consisting of frequency-tunable sub-pulses. Based on the results of cross-sectional TEM observation, we have also clarified that the EC behavior on textured glass substrates are not completely the same as that on flat glass substrates, and particularly near the glass surface, the features of crystal grains becomes different from those near the poly-Si surface.

Acknowledgment

The authors would like to thank ULVAC, Inc. for providing EB-evaporated a-Si films. This work is partly supported by JSPS Bilateral Program, Grant number JPJSBP120193511.

References

[1] M. A. Green, Crystalline and thin-film silicon solar cells: state of the art and future potential, Sol. Energy **74** (2003) 181–192.

[2] W. Fuhs, S. Gall, B. Rau, M. Schmidt, J. Schneider, A novel route to a polycrystalline silicon thin-film solar cell, Sol. Energy. **77** (2004) 961–968.

[3] M. Spitzer, J. Schewchun, E. S. Vera, J. J. Lofersky, Ultra-high efficiency thin silicon p-n junction solar cells using reflecting surfaces, Proc. 14th IEEE PV Specialists Conf., pp. 375–380, 1980.

[4] A. A. D. T. Adikaari, N. K. Mudugamuwa, S. R. P. Silva, Nanocrystalline silicon solar cells from excimer laser crystallization of amorphous silicon, Sol. Energy Mater. Sol.

Cells **92** (2008) 634–638.

[5] J. K. Saha, K. Haruta, M. Yeo, T. Koabayshi, H. Shirai, Rapid crystallization of amorphous silicon utilizing a very-high-frequency microplasma jet for Si thin-film solar cells, Sol. Energy Mater. Sol. Cells **93** (2009) 1154–1157.

[6] A. Nakajima, T. Suzuki, M. Yoshimi, K. Yamamoto, Enhancement of optical absorption for below 5 μm thin-film poly-Si solar cell on glass substrate, Sol. Energy Mater. Sol. Cells **48** (1997) 287–294.

[7] K. Yamamoto, M. Yoshimi, Y. Tawada, Y. Okamoto, A. Nakajima, S. Igari, Thin-film poly-Si solar cells on glass substrate fabricated at low temperature, Appl. Phys. A **69** (1999) 179–185.

[8] C. T. Trinh, N. Preissler, P. Sonntag, M. Muske, K. Jäger, M. Trahms, R. Schlatmann, B. Rech, D. Amkreutz, Potential of interdigitated back-contact silicon heterojunction solar cells for liquid phase crystallized silicon on glass with efficiency above 14%, Sol. Energy Mater. Sol. Cells **174** (2018) 187–195.

[9] D. Amkreutz, J. Müller, M. Schmidt, T. Hänel, T. F. Schulze, Electron-beam crystallized large grained silicon solar cell on glass substrate, Prog. Photovolt: Res. Appl. **19** (2011) 937–945.

[10] S. Garud, C. T. Trinh, D. Abou-Ras, B. Stannowski, R. Schlatmann, B. Rech, D. Amkreutz, Toward high solar cell efficiency with low material usage: 15% efficiency with 14 μm polycrystalline silicon on glass, Sol. RRL **4** (2020) 2000058.

[11] M. Miyasaka, J. Stoemenos, Excimer laser annealing of amorphous and solid-phase-crystallized silicon films, J. Appl. Phys. **86** (1999) 5556–5565.

[12] N. Matsuo, K. Uejukkoku, A. Heya, S. Amano, Y. Takanashi, S. Miyamoto, T. Mochizuki, Effect of laser-plasma X-ray irradiation on crystallization of amorphous silicon film by excimer laser annealing, Jpn. J. Appl. Phys. **46** (2007) L1061–L1063.

[13] Y. Yogoro, A. Masuda, H. Matsumura, Crystallization by excimer laser annealing for a-Si:H films with low hydrogen content prepared by Cat-CVD, Thin Solid Films **430** (2003) 296–299.

[14] F. C. Voogt, R. Ishihara, A combined TEM and time-resolved optical reflectivity investigation into the excimer-laser crystallization of a-Si films, Thin Solid Films **383** (2001) 45–47.

[15] F. C. Voogt, R. Ishihara, F. D. Tichelaar, Melting and crystallization behavior of low-pressure chemical-vapor-deposition amorphous Si films during excimer-laser annealing, J. Appl. Phys. **95** (2004) 2873–2879.

[16] R. Kakkad, J. Smith, W. S. Lau, S. J. Fonash, R. Kerns, Crystallized Si films by low-temperature rapid thermal annealing of amorphous silicon, J. Appl. Phys. **65** (1989) 2069–2072.

[17] R. Kakkad, G. Liu, S. J. Fonash, Low temperature selective crystallization of amorphous silicon, J. Non-Cryst. Solids. **115** (1989) 66–68.

[18] J. H. Choi, D. Y. Kim, S. S. Kim, S. J. Park, J. Jang, Polycrystalline silicon prepared by metal induced crystallization, Thin Solid Films **440** (2003) 1–4.

[19] A. Szekeres, M. Gartner, F. Vasiliu, M. Marinov, G. Beshkov, Crystallization of a-Si:H films by rapid thermal annealing, J. Non-Cryst. Solids **227** (1998) 954–957.

[20] G. Liu, S. J. Fonash, Selective area crystallization of amorphous silicon films by low-temperature rapid thermal annealing, Appl. Phys. Lett. **55** (1989) 660–662.

[21] F. L. Bregolin, K. Krockert, S. Prucnal, L. Vines, R. Hübner, B. G. Svensson, K. Wiesenhütter, H.-J. Möller, W. Skorupa, J. Appl. Phys. **115** (2014) 064505 .

[22] M. Shrestha, K. Wang, B. Zheng, L. Mokrzycki, Q. H. Fan, Comparative Study of Furnace and Flash Lamp Annealed Silicon Thin Films Grown by Plasma Enhanced Chemical Vapor Deposition, Coatings **8** (2018) 97.

[23] M. Smith, R. McMahon, M. Voelskow, D. Panknin, W. Skorupa, Modelling of flash-lamp-induced crystallization of amorphous silicon thin films on glass, J. Cryst. Growth **285** (2005) 249–260.

[24] K. Ohdaira, Y. Endo, T. Fujiwara, S. Nishizaki, H. Matsumura, Formation of highly uniform micrometer-order-thick polycrystalline silicon films by flash lamp annealing of amorphous silicon on glass substrates, Jpn. J. Appl. Phys. **46** (2007) 7603–7606.

[25] K. Ohdaira, T. Fujiwara, Y. Endo, S. Nishizaki, H. Matsumura, Explosive crystallization of amorphous silicon films by flash lamp annealing, J. Appl. Phys. **106** (2009) 044907.

[26] K. Ohdaira, H. Matsumura, Liquid-phase explosive crystallization of electron-beam-evaporated a-Si films induced by flash lamp annealing, J. Cryst. Growth **362** (2013) 149–152.

[27] K. Ohdaira, N. Tomura, S. Ishii, H. Matsumura, Lateral crystallization velocity in

explosive crystallization of amorphous silicon films induced by flash lamp annealing, Electrochem. Solid-State Lett. **14** (2011) H372–H374.

[28] K. Ohdaira, A method to evaluate explosive crystallization velocity of amorphous silicon films during flash lamp annealing, Can. J. Phys. **92** (2014) 718.

[29] Y. Sonoda, K. Ohdaira, Effect of anti-reflection coating on the crystallization of amorphous silicon films by flash lamp annealing, Jpn. J. Appl. Phys. **56** (2017) 04CS10.

[30] K. Kurata, K. Ohdaira, Crystallization of electron-beam evaporated a-Si films on textured glass substrates by flash lamp annealing, Jpn. J. Appl. Phys. **58** (2019) SBBF10.

[31] I. De Wolf, Micro-Raman spectroscopy to study local mechanical stress in silicon integrated circuits, Semicond. Sci. Technol. **11** (1996) 139–154.

[32] H. -D. Geiler, E. Glaser, G. Götz, M. Wagner, Explosive crystallization in silicon, J. Appl. Phys. **59** (1986) 3091.

Figure Captions

Fig. 1. (Color online) AFM images of the surfaces of glass substrates (a) before and (b) after RIE.

Fig. 2. (Color online) Optical reflectance spectra of Si films on flat and textured glass substrates before and after FLA.

Fig. 3. (Color online) Raman spectra of Si films after FLA. (a), (b), and (c) shown in the inset indicate measurement points of Raman spectra. Dash and solid lines exhibit the spectra of Si films on flat and textured glass substrates, respectively. The spectra of Si films before FLA are also shown as black lines for comparison.

Fig. 4. (Color online) Surfaces of Si films on flat and textured glass substrates after FLA with the sub-pulse frequencies of 2, 5, and 10 kHz.

Fig. 5. (Color online) Width of macroscopic stripe patterns on poly-Si films formed on flat and textured glass substrates as a function of the reciprocal of sub-pulse emission frequency. The straight lines are the results of line fitting.

Fig. 6. (Color online) Cross-sectional TEM image of a poly-Si film formed on a textured glass substrate. The cross-section was formed along an EC direction.

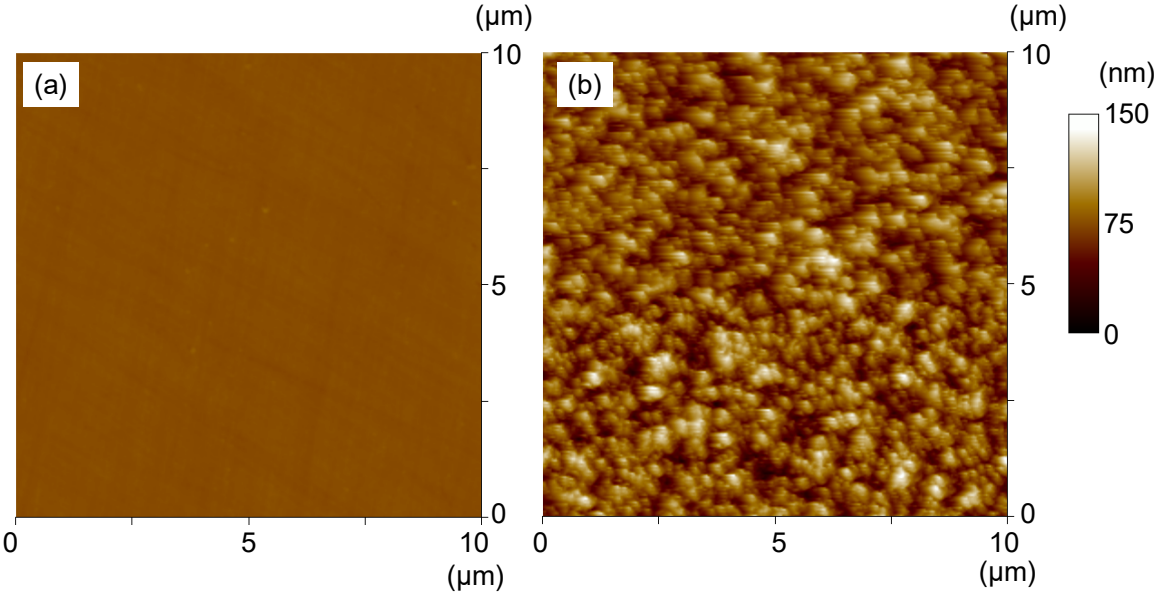
(a)
(b)
(μm)
10
5
0
0
5
10
(μm)
(nm)
150
75
0

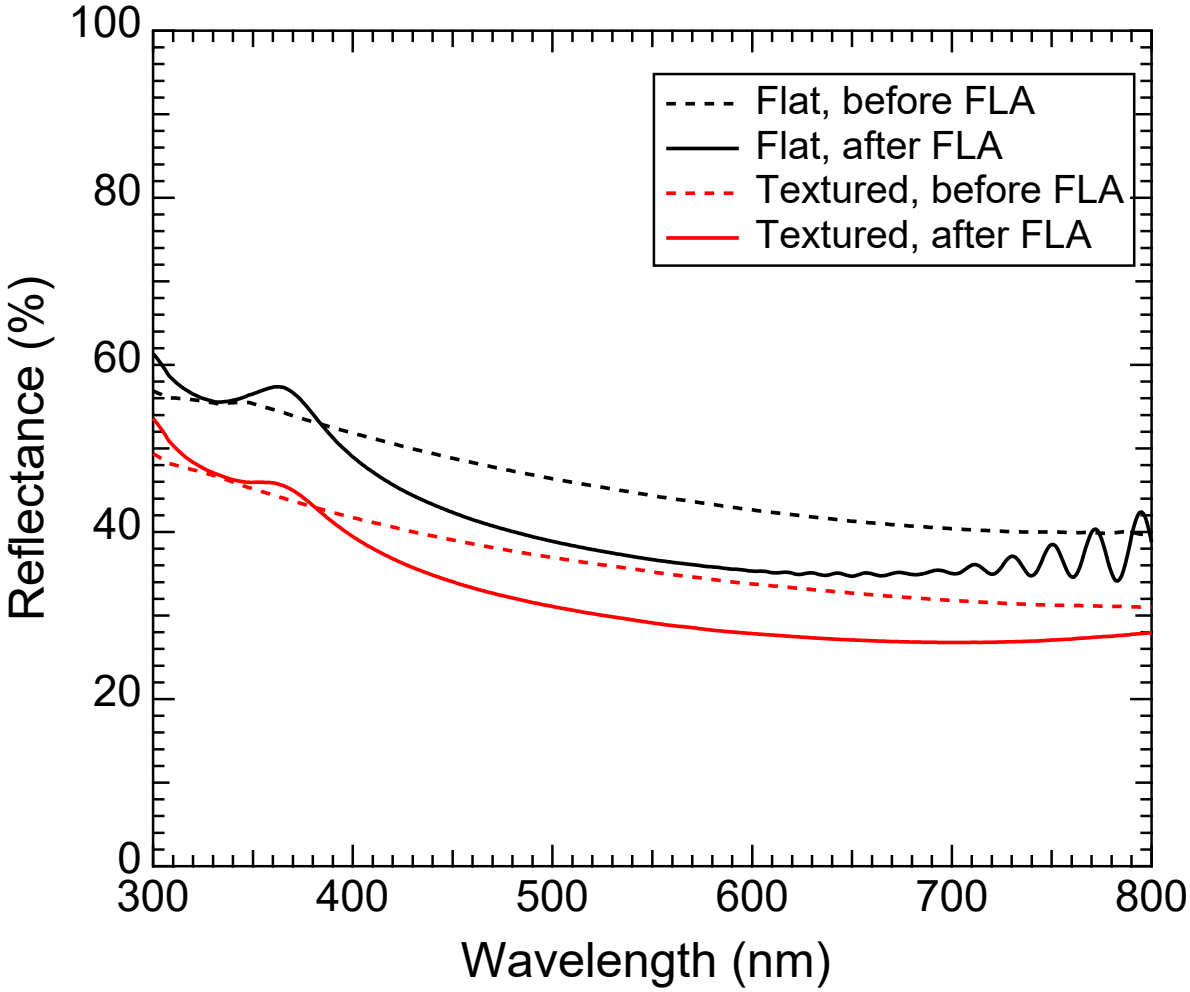
Flat, before FLA
Flat, after FLA
Textured, before FLA
Textured, after FLA
Reflectance (%)
Wavelength (nm)
0
20
40
60
80
100
300
400
500
600
700
800

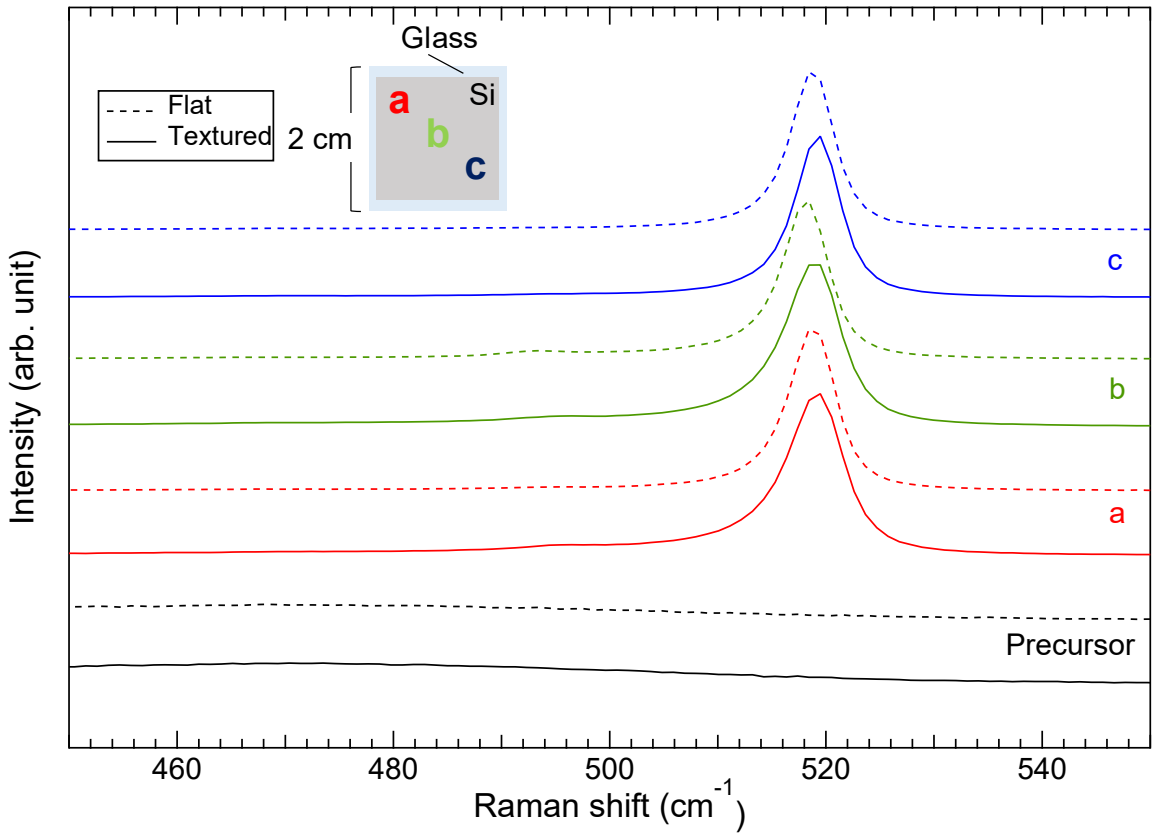
Glass
Si
a
b
c
Flat
Textured
2 cm
c
b
a
Precursor
Intensity (arb. unit)
460
480
500
520
540
Raman shift (cm-1)

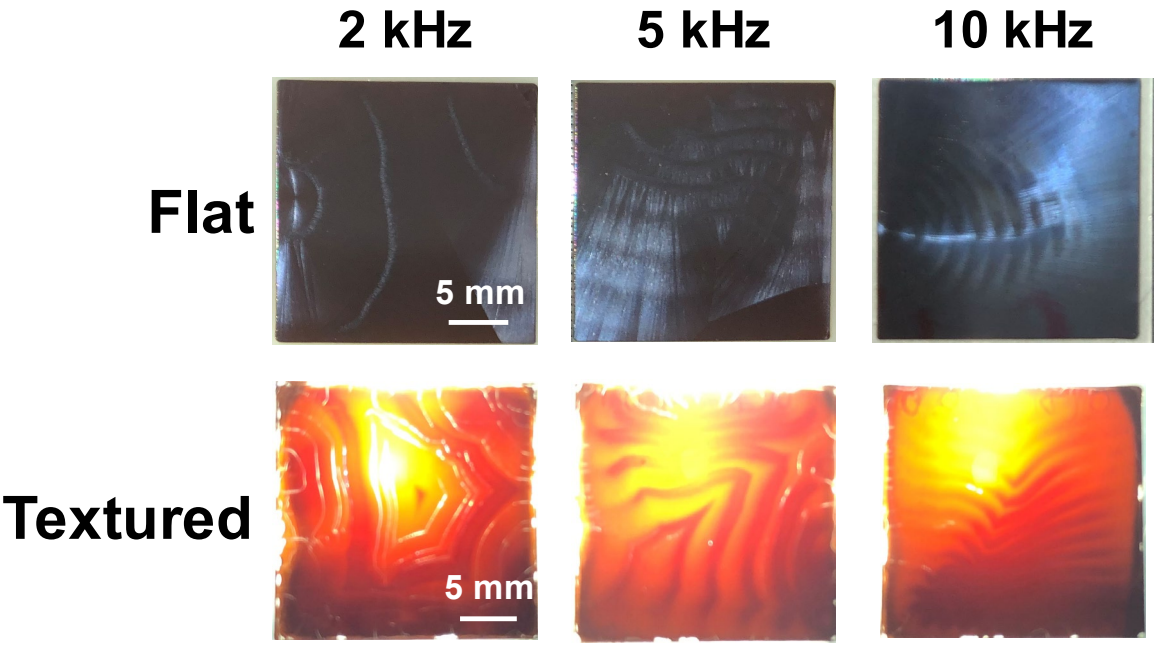
2 kHz
5 kHz
10 kHz
Flat
Textured
5 mm
5 mm

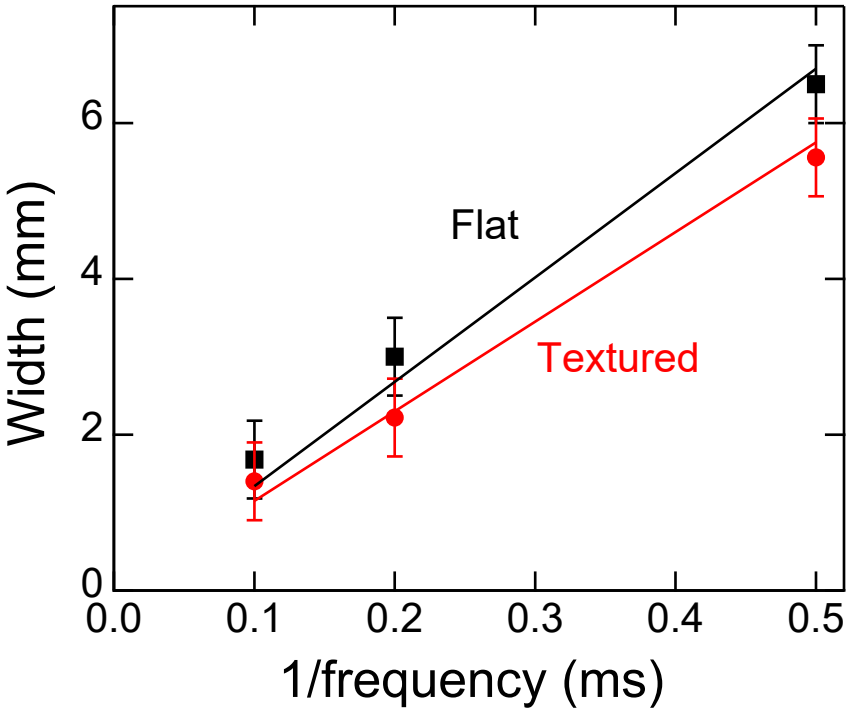
Width (mm)
0
2
4
6
0.0
0.1
0.2
0.3
0.4
0.5
1/frequency (ms)
Flat
Textured

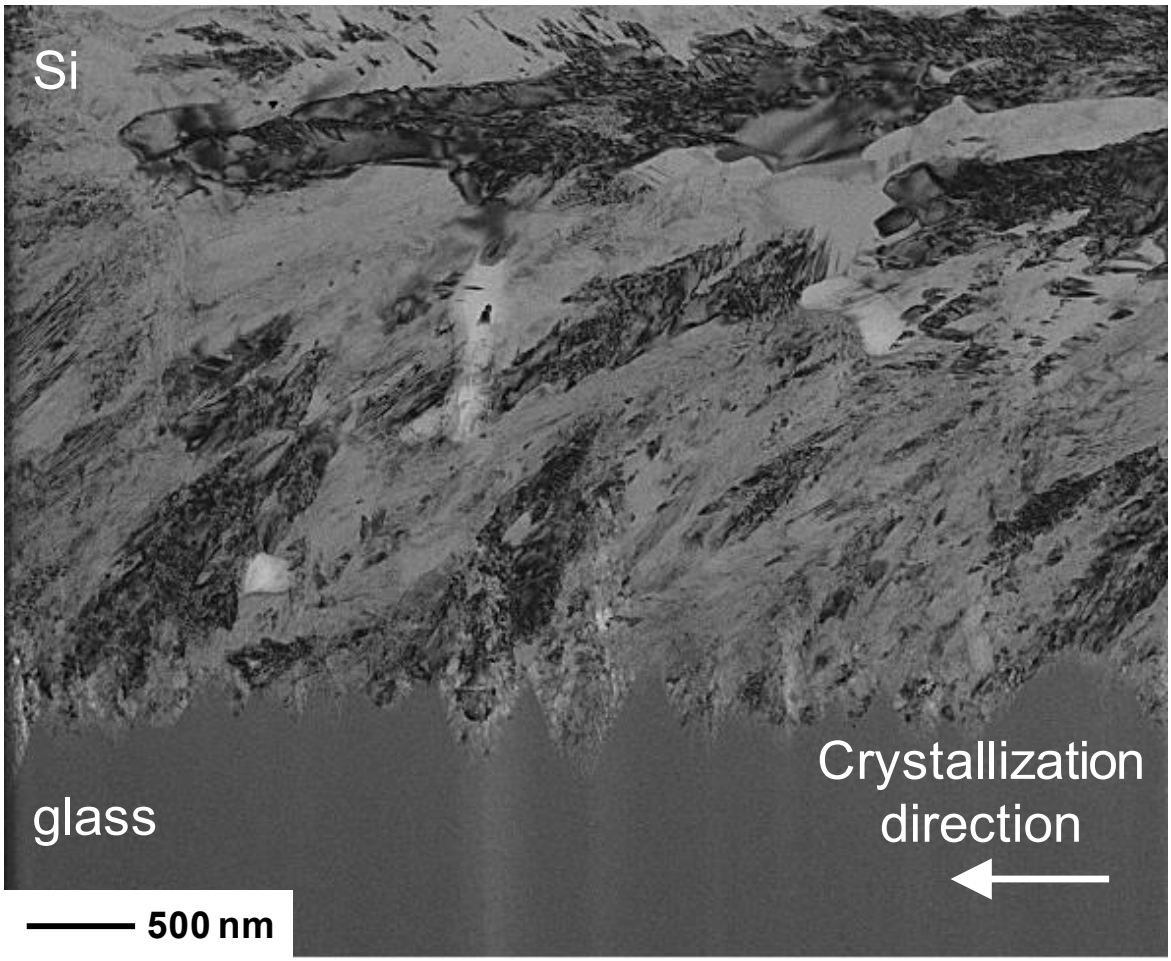
Si
glass
Crystallization
direction
500 nm